European Journal of Medicinal Chemistry 46 (2011) 3410–3419

Contents lists available at ScienceDirect

European Journal of Medicinal Chemistry

journal homepage: http://www.elsevier.com/locate/ejmech

Original article

A class of Trp-Trp-AA-OBzl: Synthesis, *in vitro* anti-proliferation/*in vivo* anti-tumor evaluation, intercalation-mechanism investigation and 3D QSAR analysis

Xiaoyi Zhang, Yifan Yang, Ming Zhao**, Liu Liu, Meiqing Zheng, Yuji Wang, Jianhui Wu, Shiqi Peng*

College of Pharmaceutical Sciences, Capital Medical University, No. 10, Beijing 100069, PR China

ARTICLE INFO

Article history:
Received 26 November 2010
Received in revised form
20 April 2011
Accepted 2 May 2011
Available online 12 May 2011

Keywords:
Trp-Trp-AA-OBzl
Anti-tumor
Intercalation
Docking
3D QSAR

ABSTRACT

From the anti-tumor active N-tryptophanyl-β-carboline-3-carboxylic acid benzyl ester and β-carboline-3-carbonyltryptophan benzyl ester, a pharmacophore, Trp-Trp-OBzl, was drawn. Based on the DOCK scores amino acid residue was inserted into the C-terminus of Trp-Trp-OBzl and twenty Trp-Trp-AA-OBzls (AA = amino acid residues) were provided as DNA intercalators. On the *in vitro* and *in vivo* models seventeen Trp-Trp-AA-OBzls were anti-tumor active, and twelve Trp-Trp-AA-OBzls were more active than cytarabine. In acute toxicity assay Trp-Trp-AA-OBzls did not damage the immunologic function and had an LD_{50} of more than 500 mg/kg. The relationships of structure and activity were analyzed with 3D QSAR. The action mechanism studies revealed that the *in vivo* anti-tumor action of Trp-Trp-AA-OBzls was the result of DNA intercalation.

1. Introduction

For some anti-tumor agents such as groove binders, alkylating compounds and intercalating agents, the DNA recognition is a critical step in their anti-tumor action. The intercalation is not only one kind of the interactions in DNA recognition but also a pivotal step of several clinically used anti-tumor drugs such as anthracyclines, acridines and anthraquinones [1]. To push clinical cancer therapy, the discovery of new DNA intercalators has been considered a practical approach. A number of intercalators such as harmines have been reported [2–4]. Harmine and its derivatives belong to β-carboline intercalators and were characterized by their cytotoxicity [5,6]. Via intercalation they are able to inhibit topoisomerases I/II and finally damage DNA. In our ongoing efforts a series of β-carboline-3-carbonylamino acid benzyl esters were presented by mimicking the natural products with potent anti-tumor activity. It was demonstrated that their *in vitro* cytotoxicity depended on the building blocks, i.e. β-carboline-3-carboxylic acid, amino acid and benzyl moieties [7]. These requirements were generally met in the design of N-(3-carboxyl-9-benzylcarboline-1-yl) ethylamino acids. The docking studies demonstrated that their *in vitro* anti-proliferation and *in vivo* anti-tumor activities could be predicted with the DOCK scores [8].

It is well documented that Trp-Trp is biologically important either as a dipeptide or as a fragment of some peptides [8,10]. For instance, via a similar ring-opening modification both the anti-tumor active β-carboline-3-carboxyltryptophan benzyl ester and N-trytophanyl-β-carboline-3-carboxylic acid benzyl ester forms Trp-Trp-OBzl (Fig. 1). This suggests that Trp-Trp-OBzl is their pharmacophore. In this context, Trp-Trp-OBzl was used as a lead, and twenty novel tripeptide benzyl esters, Trp-Trp-AA-OBzl, were provided as the DNA intercalators.

2. Results and discussion

2.1. Docking of Trp-Trp-AA-OBzl toward d(CGATCG)$_2$

DNA intercalators have been widely noticed [9–11], and the LigandFit/LigandScore in DS Modeling2.1 and d(CGATCG)$_2$ (from Protein Data Bank, 1D12) have been widely used to carry out the automated docking studies of the intercalators [9–16]. To evaluate the possibility of Trp-Trp-AA-OBzl (**4a**–**t**) as DNA intercalators an automated docking of **4a**–**t** toward the cavity of d(CGATCG)$_2$ was performed by following a general procedure, the DOCK scores were calculated and are listed in Table 1. It is shown that the DOCK scores of Trp-Trp-AA-OBzls are 31–62, and ten of them are 51–62. While our previous work indicated that the DOCK scores of the intercalators with high *in vivo* anti-tumor activity were 50–60 [8,10]. This means that at least ten Trp-Trp-AA-OBzls possibly have high *in vivo* anti-tumor activity.

* Corresponding author. Tel./fax: +86 10 8391 1528.
** Corresponding author. Tel./fax: +86 10 8280 2482.
E-mail address: sqpeng@mail.bjmu.edu.cn (S. Peng).

0223-5234/$ – see front matter © 2011 Elsevier Masson SAS. All rights reserved.
doi:10.1016/j.ejmech.2011.05.004

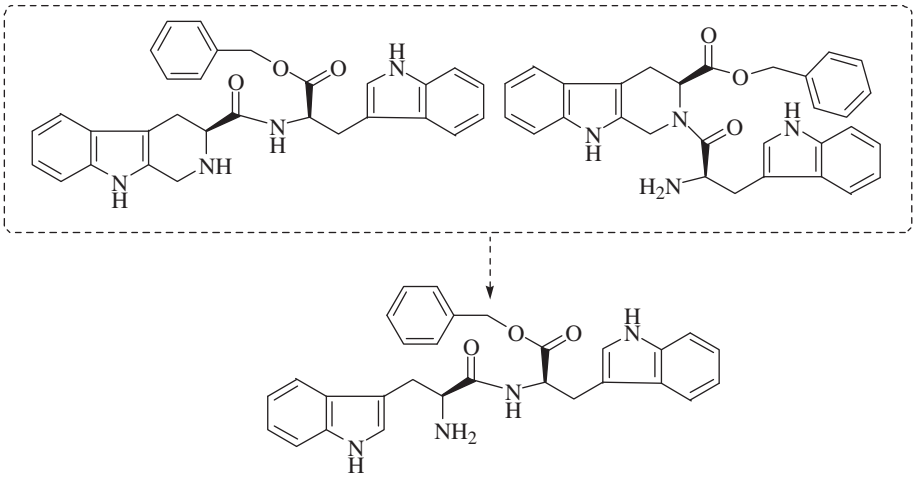

Fig. 1. Structural correlation of the derivatives of 2-Trp and 3-Trp modified β-carboline-3-carboxylic acid benzyl ester with Trp-Trp-OBzl.

2.2. Synthesis of Trp-Trp-AA-OBzl

Trp-Trp-AA-OBzls (**4a**–**t**, AA = L-amino acid residues) were prepared according to the route depicted in Scheme 1. When Boc-Trp was coupled with Trp-OBzl the protective dipeptide Boc-Trp-Trp-OBzl (**1**) was obtained (96% yield). In aqueous NaOH (2 M) the benzyl group of **1** was removed and Boc-Trp-Trp (**2**) was provided in 90% yield. The coupling reaction of Boc-Trp-Trp with AA-OBzl provided Boc-Trp-Trp-AA-OBzls (**3a**–**t**, 41%–98% yields). In the solution of hydrogen chloride in ethyl acetate the Boc groups of **3a**–**t** were removed, Trp-Trp-AA-OBzls (**4a**–**t**) were obtained and the yields were 70%–99%. To ensure the purity, **3a**–**t** were purified on a chromatographic column, while **4a**–**t** were purified by repeatedly using ether-promoted solidification and the HPLC purities were more than 97%. These data demonstrate that the used procedures and conditions are suitable for preparing of Trp-Trp-AA-OBzls in high quality and acceptable yield.

Table 1
DOCK scores of Trp-Trp-AA-OBzl (**4a**–**t**) toward $d(CGATCG)_2$.

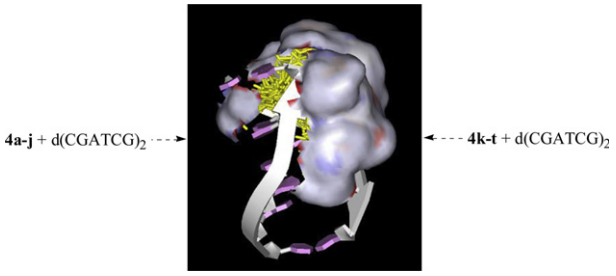

Trp-Trp-AA-OBzl/AA	DOCK score	Trp-Trp-AA-OBzl/AA	DOCK score
4a/Ala	55.6	**4k**/Met	32.1
4b/Gly	55.5	**4l**/Glu	51.2
4c/Phe	53.0	**4m**/Asp	37.4
4d/Leu	30.7	**4n**/Cys	59.6
4e/Ile	51.7	**4o**/Arg	43.0
4f/Val	61.1	**4p**/Lys	40.7
4g/Ser	39.5	**4q**/Gln	62.1
4h/Thr	58.6	**4r**/Asn	49.4
4i/Tyr	32.1	**4s**/His	38.4
4j/Pro	56.5	**4t**/Trp	41.0

2.3. Anti-proliferation activities of *4a–t*

To evaluate the *in vitro* anti-proliferation activities of **4a**–**t** the carcinoma cell lines, $HepG_2$ (human hepatocellular liver carcinoma cell line), S180 (mouse sarcoma cell line), H22 (mouse hepatocellular carcinoma cell line), K562 (human immortalized myelogenous leukemia line) and B16 (mouse melanoma cell line), were used. In the assays the cells were exposed to **4a**–**t**, cytarabine and doxorubicin (positive control), underwent the standard MTT tests and gave their proliferation inhibitions for calculate IC_{50} velues (Table 2). It can be seen that **4a**–**t** possess distinct *in vitro* anti-proliferation activities, the IC_{50} values are 8.1 μM–154.0 μM, most of them are able to inhibit the proliferation of the carcinoma cells, the IC_{50} values of **4a**–**c**,**e**,**f**,**h**,**j**,**l**,**n**,**o**,**q**,**r** are significantly lower than that of cytarabine, and the IC_{50} value of **4s** is equal to that of cytarabine. Beside, the IC_{50} values of **4a**–**f**,**h**,**j**,**l**,**n**,**o**,**q**–**s** against S180 are significantly lower than that of doxorubicin, the IC_{50} values of **4b**,**c**,**e**,**f**,**h**,**j**,**l**,**n**,**q**,**r** against K562 are significantly lower than that of doxorubicin, the IC_{50} values of **4c**,**f**,**h**,**j**,**n**,**q** against B16 are significantly lower than that of doxorubicin, the IC_{50} values of **4a**–**c**,**e**,**f**,**h**,**j**,**l**,**n**,**o**,**q**–**s** against H22 are significantly lower than that of doxorubicin, and the IC_{50} values of **4f**,**h**,**j**,**n**,**q** against HepG2 are significantly lower than that of doxorubicin. These suggest that the lead, Trp-Trp-OBzl, works well, and inserting an amino acid residue into its C-terminus influences on the *in vitro* efficacy.

2.4. Tumor weights of *4a–t* treated S180 mice

The *in vivo* anti-tumor activities of **4a**–**t** were represented with the tumor weights of the treated mice. Via the *in vivo* assays the

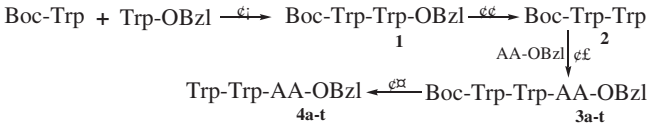

Scheme 1. Synthetic route of Trp-Trp-AA-OBzl. i) DCC, HOBt and NMM; ii) Aqueous solution of NaOH (2 M); iii) DCC, HOBt and NMM; iv) Hydrogen chloride in ethyl acetate (4 M). In **3a** & **4a** AA = Ala, **3b** & **4b** AA = Gly, **3c** & **4c** AA = Phe, **3d** & **4d** AA = Leu, **3e** & **4e** AA = Ile, **3f** & **4f** AA = Val, **3g** & **4g** AA = Ser, **3h** & **4h** AA = Thr, **3i** & **4i** AA = Tyr, **3j** & **4j** AA = Pro, **3k** & **4k** AA = Met, **3l** & **4l** AA = Glu(OBzl), **3m** & **4m** AA = Asp(OBzl), **3n** & **4n** AA = Cys(4-MeOBzl), **3o** & **4o** AA = N^G-NO_2-Arg, **3p** & **4p** AA = N^{ω}-CBz-Lys, **3q** & **4q** AA = Gln, **3r** & **4r** AA = Asn, **3s** & **4s** AA = His, **3t** & **4t** AA = Trp.

Table 2
IC_{50} (μM) of **4a**–**t** inhibiting carcinoma cell lines.[a]

Compd.	S180	K562	B16	H22	HepG2
Cytarabine	25.43 ± 1.64	24.29 ± 1.60	30.62 ± 3.14	25.98 ± 1.60	26.23 ± 1.77
Doxorubicin	29.2 ± 6.02	17.23 ± 1.43	21.50 ± 1.86	36.51 ± 3.56	17.54 ± 1.75
4a	18.52 ± 1.39[b]	18.37 ± 1.69[e]	22.98 ± 1.94[d]	20.84 ± 1.95[b]	20.06 ± 1.97[d]
4b	19.50 ± 1.42[b]	16.21 ± 1.43[b]	24.30 ± 1.98[c]	22.44 ± 1.90[b]	17.76 ± 1.43[c]
4c	14.53 ± 0.99[b]	14.92 ± 1.22[b]	19.28 ± 1.48[b]	17.44 ± 1.51[b]	16.77 ± 1.40[c]
4d	118.47 ± 10.30	116.23 ± 10.33	124.06 ± 11.00	121.26 ± 10.93	122.83 ± 10.99
4e	19.21 ± 1.49[b]	19.40 ± 1.56[c]	25.93 ± 1.99[c]	21.65 ± 1.38[b]	22.23 ± 1.99[d]
4f	8.14 ± 0.98[b]	8.27 ± 0.99 [b]	11.15 ± 1.01[b]	9.97 ± 0.98[b]	9.49 ± 0.97[b]
4g	41.22 ± 3.80	41.56 ± 3.75	54.33 ± 4.11	46.33 ± 3.90	46.55 ± 3.98
4h	11.79 ± 1.02[b]	12.01 ± 1.13[b]	15.98 ± 1.34[b]	13.98 ± 1.18[b]	13.69 ± 1.19[b]
4i	35.95 ± 2.68	45.69 ± 3.37	35.97 ± 3.03	39.57 ± 3.47	43.16 ± 3.92
4j	12.50 ± 0.90[b]	12.90 ± 0.92[b]	17.23 ± 1.49[b]	15.45 ± 1.41[b]	14.73 ± 1.39[b]
4k	49.05 ± 4.10	41.58 ± 3.97	65.41 ± 5.01	49.08 ± 4.01	52.73 ± 4.94
4l	13.39 ± 0.95[b]	10.95 ± 0.99[b]	20.75 ± 1.84[d]	13.65 ± 0.96[b]	21.02 ± 1.89[d]
4m	132.01 ± 9.30	130.15 ± 9.18	152.72 ± 10.31	99.19 ± 9.17	120.78 ± 11.94
4n	9.77 ± 0.97[b]	9.92 ± 1.04[b]	13.38 ± 1.11[b]	11.96 ± 1.08[b]	11.39 ± 1.09[b]
4o	23.69 ± 1.95[c]	20.78 ± 1.77[c]	36.32 ± 2.89	25.43 ± 2.15[c]	35.90 ± 3.90
4p	32.65 ± 2.98	32.31 ± 2.99	55.70 ± 4.51	36.56 ± 3.24	30.42 ± 2.68
4q	8.74 ± 0.89[b]	8.86 ± 0.90[b]	11.95 ± 1.02[b]	10.68 ± 0.92[b]	10.16 ± 0.98[b]
4r	15.54 ± 1.05[b]	16.29 ± 1.45[b]	21.32 ± 1.89[d]	18.67 ± 1.52[b]	17.95 ± 1.48[c]
4s	26.52 ± 1.64[c]	25.33 ± 1.65[d]	31.69 ± 3.10[e]	26.97 ± 1.65[c]	27.29 ± 1.72[e]
4t	114.56 ± 8.89	125.47 ± 9.43	156.81 ± 10.00	98.14 ± 9.00	154.03 ± 10.11

[a] $n = 6$.
[b] **For S180**: Compared to cytarabine and doxorubicin $p < 0.01$; **For K562**: Compared to cytarabine and doxorubicin $p < 0.01$; **For B16**: Compared to cytarabine and doxorubicin $p < 0.01$; **For H22**: Compared to cytarabine and doxorubicin $p < 0.01$; **For HepG2**: Compared to cytarabine and doxorubicin $p < 0.01$.
[c] **For S180**: Compared to doxorubicin $p < 0.01$; **For K562**: Compared to cytarabine $p < 0.01$; **For B16**: Compared to cytarabine $p < 0.01$; **For H22**: Compared to doxorubicin $p < 0.01$ and to cytarabine $p > 0.05$; **For HepG2**: Compared to cytarabine $p < 0.01$ and to doxorubicin $p > 0.05$.
[d] **For K562**: Compared to cytarabine $p > 0.05$; **For B16:** Compared to cytarabine $p < 0.01$ and to doxorubicin $p > 0.05$; **For HepG2**: Compared to cytarabine $p < 0.01$.
[e] **For K562**: Compared to doxorubicin $p > 0.05$; **For B16**: Compared to cytarabine $p > 0.05$; **For HepG2**: Compared to cytarabine $p > 0.05$.

tumor weights of **4a**–**t** treated S180 mice were obtained and are shown in Table 3. When the mice were given a daily i.p injection of 8.9 μmol/kg of **4a**–**t** for seven consecutive days, seventeen tripeptides (**4a**–**c**,**e**–**l**,**n**–**s**) were anti-tumor active (the tumor weights of the treated mice were 0.170 g–0.688 g were significantly lower than that, 0.827 g, of NS treated mice), and three tripeptides (**4d**,**m**,**t**) were anti-tumor inactive. Among the anti-tumor active tripeptides the efficacies of three tripeptides (**4i**,**p**,**s**, tumor weights were 0.544 g–0.660 g) were essentially equal to that of cytarabine (positive control, tumor weight 0.563 g), the efficacies of twelve tripeptides (**4a**–**c**,**e**,**f**,**h**,**j**,**l**,**n**,**o**,**q**,**r**, tumor weights were 0.170–0.434 g) were significantly higher than that of cytarabine. Besides, among the anti-tumor active tripeptides the efficacies of three tripeptides (**4e**,**o**,**r**, tumor weights were 0.401–0.434 g) were essentially equal to that of doxorubicin (positive control, tumor weight 0.429 g), the efficacies of eight tripeptides (**4b**,**c**,**f**,**h**,**j**,**l**,**n**,**q**, tumor weights were 0.170–0.359 g) were significantly higher than that of doxorubicin. These suggest that the lead, Trp-Trp-OBzl, works well, and inserting an amino acid residue into its C-terminus influences on the *in vivo* efficacy.

2.5. Effect of *4a*–*t* on the organ and body weights of treated S180 mice

The spleen index and the body weight are the important parameters to evaluate the immunologic function of the treated mice. To know the immunologic function of **4a**–**t** treated S180 mice the spleen indexes and the increased body weights were measured and are listed in Table 4. The data indicate that the liver, brain and kidney weights as well as the spleen indexes of **4a**–**t** treated S180

Table 3
Effects of **4a**–**t** on tumor weights of S180 mice.[a]

Compd	Tumor weight	Inhibition%	Compd	Tumor weight	Inhibition%
NS	0.827 ± 0.165	0.00	Cytarabine	0.563 ± 0.102	31.93 ± 5.59
4a	0.413 ± 0.087[d]	50.05 ± 7.06	Doxorubicin	0.429 ± 0.011	48.22 ± 1.20
4b	0.359 ± 0.078[e]	56.56 ± 6.64	**4l**	0.370 ± 0.063[f]	55.32 ± 7.91
4c	0.358 ± 0.077[e]	56.73 ± 6.40	**4m**	1.037 ± 0.200	−30.68 ± 4.10
4d	0.800 ± 0.157	3.29 ± 0.52	**4n**	0.300 ± 0.054[e]	63.71 ± 4.54
4e	0.401 ± 0.080[d]	51.47 ± 6.12	**4o**	0.434 ± 0.079[d]	47.51 ± 5.01
4f	0.170 ± 0.035[e]	79.45 ± 9.07	**4p**	0.544 ± 0.111[c]	34.30 ± 4.82
4g	0.678 ± 0.129[b]	18.06 ± 2.82	**4q**	0.231 ± 0.046[e]	72.03 ± 6.98
4h	0.321 ± 0.066[e]	61.25 ± 5.06	**4r**	0.409 ± 0.083[d]	50.59 ± 6.35
4i	0.660 ± 0.073[b]	20.24 ± 3.23	**4s**	0.573 ± 0.112[c]	30.69 ± 4.31
4j	0.348 ± 0.070[e]	57.98 ± 5.88	**4t**	0.985 ± 0.176	−19.07 ± 4.01
4k	0.688 ± 0.127[b]	16.86 ± 1.91			

[a] Dose = 8.9 μmol/kg, $n = 12$, tumor weight is expressed by $\bar{x} \pm$ SD g.
[b] Compared to NS $p < 0.05$.
[c] Compared to NS $p < 0.01$.
[d] Compared to NS and cytarabine $p < 0.01$, to doxorubicin $p > 0.05$.
[e] Compared to NS, cytarabine and doxorubicin $p < 0.01$.
[f] Compared to NS and cytarabine $p < 0.01$, to doxorubicin $p < 0.05$.

mice are substantially equal to those of NS, cytarabine and doxorubicin treated S180 mice, but the increased body weights of **4a**–**c**,**e**–**j**,**n**–**s** treated S180 mice are significantly higher than that of NS, cytarabine and doxorubicin treated S180 mice. The significant differences in the increased body weights demonstrate that the damage resulted from the therapy of **4a**–**c**,**e**–**j**,**n**–**s** is lower than that from the therapy of NS, cytarabine and doxorubicin.

2.6. Dose dependent in vivo anti-tumor activities of *4f*

The most potent tripeptide (**4f**) was selected to examine the dose dependent action of **4a**–**t**. At the doses of 8.9, 0.89 and 0.089 μmol/kg, **4f** showed tumor inhibitions of 79.5%, 70.2%, and 41.7%, respectively (Table 5). Therefore, **4f** possesses dose-dependent anti-tumor action.

2.7. Acute toxicity of *4a*–*c*,*e*–*l*,*n*–*s* treated mice

A series of intercalators were known to be strong neurotoxic [17]. To know the toxicity of Trp-Trp-AA-OBzl the anti-tumoral active **4a**–**c**,**e**–**l**,**n**–**s** were examined for the LD_{50} and neurotoxicity in mouse model. The examination indicates that even receiving 500 mg/kg of **4a**–**c**,**e**–**l**,**n**–**s** the mice neither exhibit tremor, twitch, jumping, tetanus, and supination, nor occur death. On the 7th day the necropsy findings in 500 mg/kg of **4a**–**c**,**e**–**l**,**n**–**s** receiving mice revealed that the therapy led no apparent changes in any organs. These suggest that **4a**–**c**,**e**–**l**,**n**–**s** are comparatively non-toxic, and their LD_{50} values should be more than 500 mg/kg.

2.8. Action mechanism of *4f*

Small molecule induced variation of UV, circular dichroic (CD), fluorescence, viscosity and melting temperature has been widely used to identify DNA intercalation [18–21]. In the examination of the intercalation of **4a**–**t** toward DNA calf thymus DNA (CT DNA) was used as the model DNA and **4f** was used as model tripeptide, and the viscosity and melting temperature of CT DNA alone were compared to those of CT DNA plus **4f**.

Table 5
Anti-tumor activity of **4f** at different doses against S180 mice.[a]

Compd.	Dose (μmol/kg)	Tumor weight (g)	%Inhibition
Cytarabine	8.9	0.563 ± 0.102[b]	31.93 ± 5.59
	0.89	0.657 ± 0.113[c]	20.57 ± 3.02
	0.089	0.762 ± 0.129	7.86 ± 1.18
4f	8.9	0.170 ± 0.035[d]	79.45 ± 9.07
	0.89	0.246 ± 0.044[e]	70.23 ± 6.07
	0.089	0.482 ± 0.049[f]	41.72 ± 4.39
NS	0.2 ml	0.827 ± 0.165	

[a] $n = 12$, tumor weight is expressed by $\bar{x} \pm$ SD g.
[b] Compared to 0.89 μmol/kg of cytarabine $p < 0.05$.
[c] Compared to 0.089 μmol/kg of cytarabine $p < 0.05$.
[d] Compared to 0.89 μmol/kg of **4f** and 8.9 μmol/kg of cytarabine $p < 0.01$.
[e] Compared to 0.089 μmol/kg of **4f** and 8.9 μmol/kg of cytarabine $p < 0.01$.
[f] Compared to NS and 0.89 μmol/kg of cytarabine $p < 0.01$.

2.8.1. Viscosity of CT DNA without and with *4f*

In the intercalation in order to accommodate and bind small molecule the base pairs of the DNA can be pushed apart and consequently could result in the increase of the viscosity. Thus the increase of the viscosity has been widely used to reflect the intercalation [19,20]. Herein the relative viscosities of the sample solutions of [**4f**]/[CT DNA] in the ratios of 0–0.36 were measured. Fig. 2 explains that the relative viscosity of CT DNA is gradually increased with the increase of the concentration of **4f** added. This is in consistent with the intercalation of **4f** toward CT DNA.

2.8.2. Melting temperature of CT DNA without and with *4f*

The thermal melting of DNA is widely used to measure the thermostability of the double helix [21,22]. If the buffer solution of DNA was heated at a properly elevated temperature its double strands will dissociate, the corresponding single stands will form, and the absorbance of the solution will increase. The temperature that induces the absorbance of DNA solution a 50% increase is termed melting temperature (Tm). Here the temperature of the solution of CT DNA alone (PBS, pH 7.4, 100 μM) and it plus **4f** (PBS, pH 7.4, 18 μM) was risen at a rate of 1 °C/min and the absorbance was monitored at 279 nm. The melting curves of CT DNA alone and CT DNA plus **4f** are shown with Fig. 3. The fact that the Tm of CT

Table 4
Effect of **4a**–**t** on the spleen index and organ weights of S180 mice.[a]

Compd.	Liver	Brain	Kidney	Spleen index	Increased BW
NS	1.85 ± 0.23	0.27 ± 0.03	0.16 ± 0.02	7.26 ± 1.37	8.42 ± 1.52
Cytarabine	1.62 ± 0.11	0.29 ± 0.02	0.16 ± 0.03	7.50 ± 1.84	7.12 ± 1.39
Doxorubicin	1.61 ± 0.06	0.25 ± 0.01	0.15 ± 0.02	7.31 ± 1.61	6.12 ± 1.39
4a	1.77 ± 0.13[b]	0.27 ± 0.03	0.16 ± 0.01	7.59 ± 1.38	9.50 ± 1.05[b]
4b	1.80 ± 0.21[b]	0.27 ± 0.02	0.16 ± 0.02	8.11 ± 1.39	9.77 ± 1.25[b]
4c	1.89 ± 0.21[b]	0.28 ± 0.03	0.16 ± 0.01	7.96 ± 1.36	9.86 ± 1.22[b]
4d	1.70 ± 0.17	0.26 ± 0.02	0.16 ± 0.02	7.45 ± 1.80	8.40 ± 1.45
4e	1.85 ± 0.19[b]	0.28 ± 0.03	0.17 ± 0.02	8.12 ± 1.66	9.80 ± 1.39[b]
4f	1.89 ± 0.20[b]	0.27 ± 0.01	0.15 ± 0.02	7.97 ± 1.63	9.97 ± 1.39[b]
4g	1.73 ± 0.20	0.28 ± 0.05	0.16 ± 0.02	7.59 ± 1.96	9.95 ± 1.33[b]
4h	1.81 ± 0.05[b]	0.30 ± 0.07	0.15 ± 0.02	8.21 ± 1.55	9.99 ± 1.38[b]
4i	1.78 ± 0.19[b]	0.27 ± 0.03	0.16 ± 0.03	7.50 ± 1.84	9.76 ± 1.40[b]
4j	1.81 ± 0.20[b]	0.27 ± 0.01	0.15 ± 0.01	8.01 ± 1.79	10.24 ± 1.64[b]
4k	1.74 ± 0.25	0.28 ± 0.03	0.16 ± 0.03	7.69 ± 1.88	8.93 ± 1.55[c]
4l	1.86 ± 0.13[b]	0.27 ± 0.02	0.17 ± 0.02	7.92 ± 1.60	9.94 ± 1.43[b]
4m	1.77 ± 0.15[b]	0.27 ± 0.03	0.15 ± 0.02	8.25 ± 1.78	8.38 ± 1.17
4n	1.75 ± 0.143	0.27 ± 0.01	0.16 ± 0.03	8.21 ± 1.66	9.69 ± 1.04[b]
4o	1.87 ± 0.27[b]	0.27 ± 0.01	0.16 ± 0.02	7.99 ± 1.82	9.93 ± 1.46[b]
4p	1.88 ± 0.27[b]	0.27 ± 0.02	0.16 ± 0.02	8.22 ± 1.60	9.76 ± 1.31[b]
4q	1.81 ± 0.18[b]	0.27 ± 0.01	0.16 ± 0.02	7.96 ± 1.90	9.89 ± 1.49[b]
4r	1.82 ± 0.16[b]	0.27 ± 0.01	0.16 ± 0.02	7.81 ± 1.32	9.96 ± 1.41[b]
4s	1.78 ± 0.22[b]	0.28 ± 0.02	0.16 ± 0.02	8.34 ± 1.40	10.04 ± 1.49[b]
4t	1.78 ± 0.21[b]	0.29 ± 0.03	0.16 ± 0.02	7.75 ± 1.72	8.71 ± 1.50[c]

[a] Dose = 8.9 μmol/kg, BW = body weight, body and organ weights are expressed by $\bar{x} \pm$ SD g $n = 12$.
[b] **For liver weight**: Compared to cytarabine and doxorubicin $p < 0.05$, to NS $p > 0.05$; **For increased body weight**: Compared to cytarabine and doxorubicin $p < 0.01$, to NS $p > 0.05$.
[c] **For increased body weight**: Compared to cytarabine $p < 0.01$, to doxorubicin $p < 0.01$, to NS $p > 0.05$.

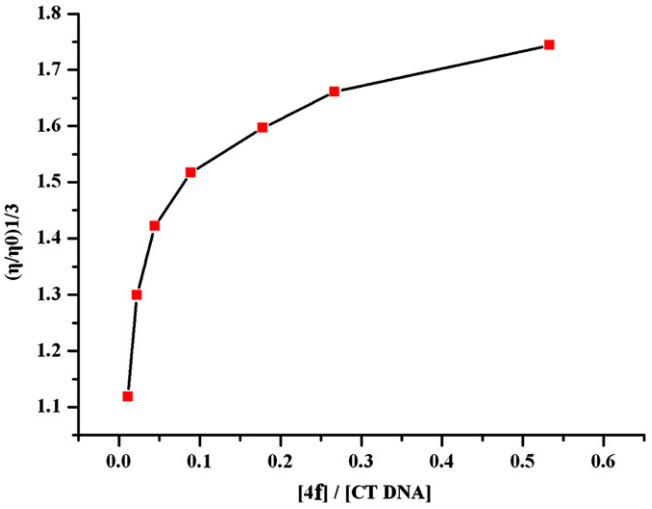

Fig. 2. Effect of **4f** on the relative viscosity of CT DNA (200 μM).

DNA plus **4f** is 22.0 ± 0.6 °C higher than that of CT DNA alone indicates that in the presence of **4f** the double strands of CT DNA are stabilized. This increased stability of the double helix of CT DNA can be attributed to the intercalation of **4f** toward CT DNA.

2.9. 3D QSAR analysis of ***4a–t***

To elucidate the effects of Trp-Trp-AA-OBzl (**4a–t**) on the tumor weights of the treated S180 mice the 3D QSAR analysis was performed. For 3D QSAR the training set **4a–n,p,r–t** and the test set **4o,q** selections were made manually such that they populated over a wide range of anti-tumor activities in a similar proportion. The 3D QSAR module of Cerius2 was followed to quantitatively correlate the tumor weights with the structures of **4a–n,p,r–t**. To obtain a consistent alignment, their common moiety, Trp-Trp, was selected as the template for superposing **4a–t**. The method used for performing the alignment was the maximum common subgraph (MCS) [23]. The stereoview of aligned **4a–t** is shown in Fig. 4. The alignment stereoview explores that to superimpose onto Trp-Trp the C-terminal amino acid residue of each structure of Trp-Trp-AA-OBzl has to take individual conformation.

Based on the alignment molecular field analysis (MFA) of **4a–n,p,r–t** was performed by using the QSAR module of Cerius2

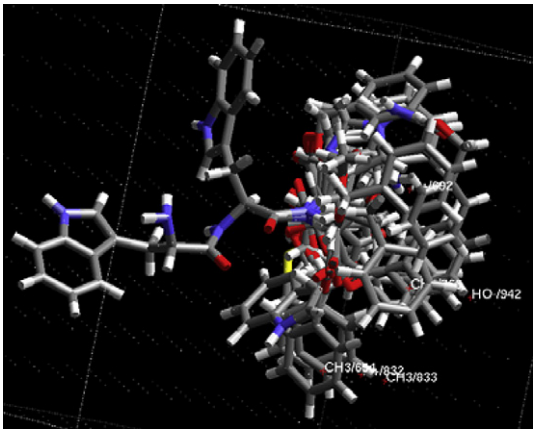

Fig. 4. Alignment stereoview of **4a–t** used for molecular field generation.

[24]. Both the electrostatic and steric fields of **4a–n,p,r–t** were created by use of proton, hydroxyl group and methyl group as the probe. These fields were sampled at each point of a regularly spaced grid of 1 Å. An energy cutoff of ±30.0 kcal/mol was set for two fields. The totally generated grid points were 1200. The regression analysis was carried out by using the genetic partial least square (G/PLS) method consisting of 10,000 generations with a population size of 100. The number of the components was set to 5. The cross-validation was performed with the leave-one-out procedure. PLS analysis was scaled, with all variables normalized to a variance of 1.0. The MFA model for the tumor weights of **4a–n,p,r–t** treated mice in terms of the most relevant descriptors including proton, hydroxyl group and methyl group is expressed by equation (1).

$$\begin{aligned}\text{Tumor weight} &= 0.13 + 0.0068\left(\mathrm{H^+}/692\right) \\ &\quad - 0.0038\left(\mathrm{H^+}/832\right) + 0.0086(\mathrm{CH_3}/654) \\ &\quad + 0.0062(\mathrm{CH_3}/763) - 0.0041(\mathrm{CH_3}/833) \\ &\quad + 0.0051\left(\mathrm{HO^-}/942\right) \qquad (1)\end{aligned}$$

The data points (n), correlation coefficient (r) and square correlation coefficient (r^2) of equation (1) were 18, 0.974 and 0.948, respectively. The correlation of the tested tumor weights on S180

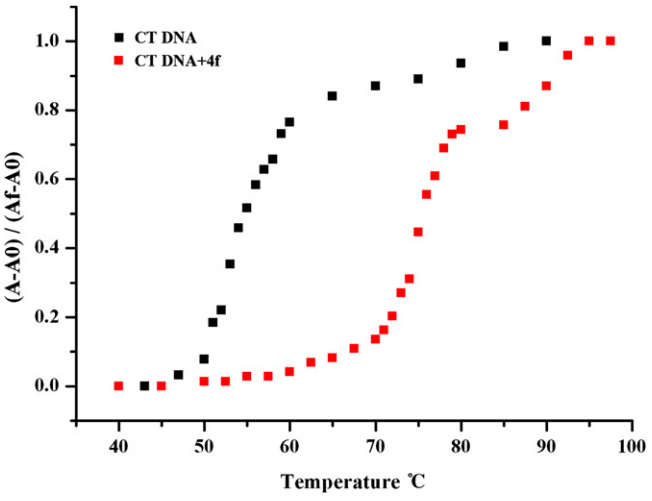

Fig. 3. Thermal denaturation curves of CT DNA without and with **4f**.

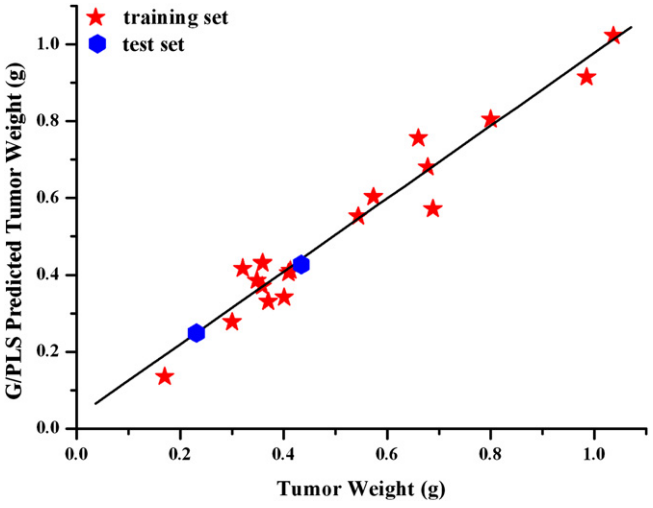

Fig. 5. Graph of the tested tumor weights against calculated tumor weights.

Table 6
Predict and test tumor weight of **4o**,**q** treated mice.

Compd.	Tumor weight (g)		
	Predict value	Test value	Error
4o	0.427	0.434	−0.007
4q	0.249	0.231	0.018

mouse model with the calculated tumor weights from equation (1) is explained with Fig. 5.

In equation (1) one term of H^+/692 with positive coefficient from proton descriptor, which means that at this position electron-releasing group will increase the *in vivo* anti-tumor activity, one term of H^+/832 with negative coefficient from proton descriptor, which means that at this position electron-releasing group will decrease the *in vivo* anti-tumor activity, two terms of CH_3/654 and CH_3/763 with positive coefficients from methyl descriptor, which means that at this positions large group will increase the *in vivo* anti-tumor activity, one term of CH_3/833 with negative coefficient from methyl descriptor, which means that at this positions large group will decrease the *in vivo* anti-tumor activity, and one term of HO^-/942 with positive coefficient from hydroxyl descriptor, which means that at this position hydrogen bond forming group will increase the activity, are involved.

The predict power of equation (1) was demonstrated by the comparison of the calculated and the tested tumor weights of the test set (Table 6, **4o**,**q**). The results indicate that equation (1) rationally gives the tumor weights of **4o** and **4q** treated mice and the errors are −0.007 g and 0.018 g, respectively. The calculated tumor weight closes the experimental tumor weight means that equation (1) is practical to accurately predict the anti-tumor activity of Trp-Trp-AA-OBzl.

3. Conclusions

A similar ring-opening modification of the anti-tumoral active N-tryptophanyl-β-carboline-3-carboxylic acid benzyl ester and β-carboline-3-carbonyltryptophan benzyl ester a pharmacophore, Trp-Trp-OBzl, was obtained. With Trp-Trp-OBzl as a lead and inserting amino acid residue into its C-terminus twenty anti-tumoral active tripeptides, Trp-Trp-AA-OBzls, were built. The *in vivo* anti-tumor activities of twelve of twenty Trp-Trp-AA-OBzls were higher than that cytarabine. The acute toxicity assay defined Trp-Trp-AA-OBzls having a LD_{50} value of more than 500 mg/kg. The automated docking, UV, CD, fluorescence, viscosity and melting temperature studies suggested the anti-tumor action mechanism of Trp-Trp-AA-OBzls to be DNA intercalation. The effect of C-terminal amino acid residue on the anti-tumor activity can be quantitatively estimated with 3D QSAR.

4. Experimental

4.1. General

All chemicals were purchased from commercial suppliers and were purified when necessary. Protected amino acids with L-configuration were purchased from sigma chemical Co. Chromatography was performed on Qingdao silica gel H. The purities (>97%) of the intermediates and the products were measured by TLC analysis (Merck silica gel plates of type 60 F_{254}, 0.25 mm layer thickness) and HPLC analysis (waters, C_{18} column, 4.6 × 150 mm). Melting points were determined in capillary tubes on an electrothermal SM/XMP apparatus and without correction. UV spectra were measured on Shimadzu UV 2550. ESI-MS was determined by Micromass Quattro micro TM API, Waters Co. ^{1}H NMR (500 Hz) and ^{13}C NMR (125 Hz) spectra were acquired on a Bruker AC 300 spectrometer in $CDCl_3$ or in DMSO-d_6 with TMS as internal standard, and chemical shifts are expressed in ppm. Optical rotations were determined with a Jasco P-1020 Polarimeter. Statistical analysis of all the biological data was carried out by use of ANOVA test, $p < 0.05$ is considered significant.

4.1.1. Boc-Trp-Trp-OBzl (**1**)

At 0 °C, 1.87 g (6.6 mmol) of 1-hydroxybenzotriazole (HOBt) and 1.48 g (7.2 mmol) of dicyclohexylcarbodiimide (DCC) were added to a solution of 2.84 g (7.2 mmol) of Boc-Trp and 2.17 g (6.6 mmol) of HCl·Trp-OBzl in 40 ml of anhydrous THF. At 0 °C the reaction mixture was adjusted pH 8 with 1.44 ml (6.6 mmol) of NMM and then stirred for 24 h. The precipitated DCU was removed by filtration. The filtrate was evaporated under reduced pressure, and the residue was dissolved in 80 ml of EtOAc. The solution was washed successively with saturated aqueous $NaHCO_3$, aqueous $KHSO_4$ (5%) and saturated aqueous NaCl. The organic phase was dried over anhydrous Na_2SO_4. After filtration and evaporation under reduced pressure, the residue was purified by column chromatography eluting with $CHCl_3$:CH_3OH (30:1) to provide 3.68 g (96%) of the title compound as colorless powder. Mp 189–191 °C, ESI/MS (*m*/*e*) 581 $[M + H]^+$.

4.1.2. Boc-Trp-Trp (**2**)

At 0 °C to the solution of 1.00 g (1.72 mmol) of Boc-Trp-Trp-OBzl in 10 ml of methanol 3 ml of aqueous NaOH (2 M) was added to adjust the solution to pH 12. The reaction mixture was stirred at 0 °C for 30 min, and then was adjusted to pH 5.5 with hydrochloric acid (2 N). After filtration the filtrate was evaporated under reduced pressure. The residue was dissolved in 30 ml of methanol and the solution was filtered. The filtrate was evaporated under reduced pressure and the residue was solidified in 10 ml of anhydrous ether to provide 0.76 g (90%) of the title compound as colorless powder. Mp 200–202 °C, ESI/MS (*m*/*e*) 491 $[M + H]^+$.

4.1.3. Boc-Trp-Trp-Ala-OBzl (**3a**)

Using the same procedure as described for Boc-Trp-Trp-OBzl from 490 mg (1.0 mmol) of Boc-Trp-Trp and 386 mg (1.1 mmol) of Tos·Ala-OBzl 641 mg (98%) of the title compound was obtained as colorless powder. Mp 202–204 °C, ESI/MS (*m*/*e*) 652 $[M + H]^+$.

4.1.4. Boc-Trp-Trp-Gly-OBzl (**3b**)

Using the same procedure as described for Boc-Trp-Trp-OBzl from 490 mg (1.0 mmol) of Boc-Trp-Trp and 371 mg (1.1 mmol) of Tos·Gly-OBzl 414 mg (65%) of the title compound was obtained as colorless powder. Mp 206–208 °C, ESI/MS (*m*/*e*) 638 $[M + H]^+$.

4.1.5. Boc-Trp-Trp-Phe-OBzl (**3c**)

Using the same procedure as described for Boc-Trp-Trp-OBzl from 490 mg (1.0 mmol) of Boc-Trp-Trp and 470 mg (1.1 mmol) of Tos·Phe-OBzl 682 mg (94%) of the title compound was obtained as colorless powder. Mp 200–202 °C, ESI/MS (*m*/*e*) 638 $[M + H]^+$.

4.1.6. Boc-Trp-Trp-Leu-OBzl (**3d**)

Using the same procedure as described for Boc-Trp-Trp-OBzl from 490 mg (1.0 mmol) of Boc-Trp-Trp and 432 mg (1.1 mmol) of Tos·Leu-OBzl 675 mg (97%) of the title compound was obtained as colorless powder. Mp 206–208 °C, ESI/MS (*m*/*e*) 694 $[M + H]^+$.

4.1.7. Boc-Trp-Trp-Ile-OBzl (**3e**)

Using the same procedure as described for Boc-Trp-Trp-OBzl from 490 mg (1.0 mmol) of Boc-Trp-Trp and 432 mg (1.1 mmol) of Tos·Ile-OBzl 687 mg (99%) of the title compound was obtained as colorless powder. Mp 212–214 °C, ESI/MS (*m*/*e*) 694 $[M + H]^+$.

*4.1.8. Boc-Trp-Trp-Val-OBzl (**3f**)*

Using the same procedure as described for Boc-Trp-Trp-OBzl from 490 mg (1.0 mmol) of Boc-Trp-Trp and 432 mg (1.1 mmol) of Tos·Val-OBzl 642 mg (95%) of the title compound was obtained as colorless powder. Mp 210–212 °C, ESI/MS (*m*/*e*) 680 $[M + H]^+$.

*4.1.9. Boc-Trp-Trp-Ser-OBzl (**3g**)*

Using the same procedure as described for Boc-Trp-Trp-OBzl from 490 mg (1.0 mmol) of Boc-Trp-Trp and 404 mg (1.1 mmol) of Tos·Ser-OBzl 563 mg (84%) of the title compound was obtained as colorless powder. Mp 195–197 °C, ESI/MS (*m*/*e*) 668 $[M + H]^+$.

*4.1.10. Boc-Trp-Trp-Thr-OBzl (**3h**)*

Using the same procedure as described for Boc-Trp-Trp-OBzl from 490 mg (1.0 mmol) of Boc-Trp-Trp and 419 mg (1.1 mmol) of Tos·Thr-OBzl 580 mg (85%) of the title compound was obtained as colorless powder. Mp 190–192 °C, ESI/MS (*m*/*e*) 682 $[M + H]^+$.

*4.1.11. Boc-Trp-Trp-Tyr-OBzl (**3i**)*

Using the same procedure as described for Boc-Trp-Trp-OBzl from 490 mg (1.0 mmol) of Boc-Trp-Trp and 487 mg (1.1 mmol) of Tos·Tyr-OBzl 708 mg (95%) of the title compound was obtained as colorless powder. Mp 220–222 °C, ESI/MS (*m*/*e*) 744 $[M + H]^+$.

*4.1.12. Boc-Trp-Trp-Pro-OBzl (**3j**)*

Using the same procedure as described for Boc-Trp-Trp-OBzl from 490 mg (1.0 mmol) of Boc-Trp-Trp and 266 mg (1.1 mmol) of HCl·Tyr-OBzl 654 mg (96%) of the title compound was obtained as colorless powder. Mp 182–184 °C, ESI/MS (*m*/*e*) 678 $[M + H]^+$.

*4.1.13. Boc-Trp-Trp-Met-OBzl (**3k**)*

Using the same procedure as described for Boc-Trp-Trp-OBzl from 490 mg (1.0 mmol) of Boc-Trp-Trp and 452 mg (1.1 mmol) of Tos·Met-OBzl 692 mg (97%) of the title compound was obtained as colorless powder. Mp 218–220 °C, ESI/MS (*m*/*e*) 712 $[M + H]^+$.

*4.1.14. Boc-Trp-Trp-Glu(OBzl)-OBzl (**3l**)*

Using the same procedure as described for Boc-Trp-Trp-OBzl from 490 mg (1.0 mmol) of Boc-Trp-Trp and 549 mg (1.1 mmol) of Tos·Glu(OBzl)-OBzl 471 mg (59%) of the title compound was obtained as colorless powder. Mp 202–204 °C, ESI/MS (*m*/*e*) 800 $[M + H]^+$.

*4.1.15. Boc-Trp-Trp-Asp(OBzl)-OBzl (**3m**)*

Using the same procedure as described for Boc-Trp-Trp-OBzl from 490 mg (1.0 mmol) of Boc-Trp-Trp and 533 mg (1.1 mmol) of Tos·Asp(OBzl)-OBzl 473 mg (60%) of the title compound was obtained as colorless powder. Mp 208–210 °C, ESI/MS (*m*/*e*) 786 $[M + H]^+$.

*4.1.16. Boc-Trp-Trp-Cys(4-MeOBzl)-OBzl (**3n**)*

Using the same procedure as described for Boc-Trp-Trp-OBzl from 490 mg (1.0 mmol) of Boc-Trp-Trp and 404 mg (1.1 mmol) of HCl·Cys(4-OMeBzl)-OBzl 801 mg (99%) of the title compound was obtained as colorless powder. Mp 221–223 °C, ESI/MS (*m*/*e*) 804 $[M + H]^+$.

*4.1.17. Boc-Trp-Trp-Arg(N^GNO_2)-OBzl (**3o**)*

Using the same procedure as described for Boc-Trp-Trp-OBzl from 490 mg (1.0 mmol) of Boc-Trp-Trp and 404 mg (1.1 mmol) of HCl·Arg(NO_2)-OBzl 317 mg (41%) of the title compound was obtained as colorless powder. Mp 207–209 °C, ESI/MS (*m*/*e*) 782 $[M + H]^+$.

*4.1.18. Boc-Trp-Trp-Lys(N^{ω}-Z)-OBzl (**3p**)*

Using the same procedure as described for Boc-Trp-Trp-OBzl from 490 mg (1.0 mmol) of Boc-Trp-Trp and 596 mg (1.1 mmol) of Tos·Lys(N^{ω}-Z)-OBzl 829 mg (98%) of the title compound was obtained as colorless powder. Mp 201–203 °C, ESI/MS (*m*/*e*) 843 $[M + H]^+$.

*4.1.19. Boc-Trp-Trp-Gln-OBzl (**3q**)*

Using the same procedure as described for Boc-Trp-Trp-OBzl from 490 mg (1.0 mmol) of Boc-Trp-Trp and 300 mg (1.1 mmol) of HCl·Gln-OBzl 469 mg (66%) of the title compound was obtained as colorless powder. Mp 195–197 °C, ESI/MS (*m*/*e*) 709 $[M + H]^+$.

4.1.20. Boc-Trp-Trp-Asn-OBzl (3r)

Using the same procedure as described for Boc-Trp-Trp-OBzl from 490 mg (1.0 mmol) of Boc-Trp-Trp and 286 mg (1.1 mmol) of HCl·Asn-OBzl 633 mg (91%) of the title compound was obtained as colorless powder. Mp 190–192 °C, ESI/MS (*m*/*e*) 695 $[M + H]^+$.

*4.1.21. Boc-Trp-Trp-His-OBzl (**3s**)*

Using the same procedure as described for Boc-Trp-Trp-OBzl from 490 mg (1.0 mmol) of Boc-Trp-Trp and 648 mg (1.1 mmol) of 2Tos·His-OBzl 556 mg (68%) of the title compound was obtained as colorless powder. Mp 189–191 °C, ESI/MS (*m*/*e*) 718 $[M + H]^+$.

*4.1.22. Boc-Trp-Trp-Trp-OBzl (**3t**)*

Using the same procedure as described for Boc-Trp-Trp-OBzl from 490 mg (1.0 mmol) of Boc-Trp-Trp and 363 mg (1.1 mmol) of HCl·Trp-OBzl 664 mg (87%) of the title compound was obtained as colorless powder. Mp 180–192 °C, ESI/MS (*m*/*e*) 767 $[M + H]^+$.

*4.1.23. Trp-Trp-Ala-OBzl (**4a**)*

To 500 mg (0.78 mmol) of Boc-Trp-Trp-Ala-OBzl 7 ml of 4 M solution of hydrochloride in ethyl acetate was added. The reaction mixture was stirred at room temperature for 60 min and TLC (chloroform/methanol, 5:1) indicated the disappearance of Boc-Trp-Trp-Ala-OBzl. The reaction mixture was evaporated under reduced pressure, the residue was dissolved in 40 ml of ethyl acetate, the solution was again evaporated under reduced pressure and the residue was washed with anhydrous ether to provide 449 mg (98%) of the title compound as colorless powder. Mp. 205–207 °C; ESI/MS (*m*/*e*) 552 $[M + H]^+$; $[\alpha]_D^{20} = 11.03$ (*c* 1, CH_3OH); ^1H NMR (500 MHz, DMSO-d_6) δ/ppm = 10.90 (m, 2H), 8.66 (d, $J = 7.3$ Hz, 1H), 8.59 (d, $J = 8.1$ Hz, 1H), 7.63 (d, $J = 7.8$ Hz, 1H), 7.49 (d, $J = 7.8$ Hz, 1H), 7.14 (m, 13H), 5.02 (m, 2H), 4.66 (m, 2H), 4.60 (m, 1H), 3.10 (m, 4H), 2.03 (s, 2H), 1.49 (m, 3H); ^{13}C NMR (125 MHz, DMSO-d_6) δ/ppm = 172.9, 142.3, 136.7, 130.1, 127.7, 127.5, 127.2, 122.9, 122.2, 120.1, 119.2, 119.0, 111.3, 111.1, 110.9, 68.5, 54.6, 48.7, 31.4, 30.7, 20.5. Anal. Calcd for $C_{32}H_{33}N_5O_4$: C, 69.67; H, 6.03; N, 12.70. Found: C, 69.88; H, 6.17; N, 12.91.

*4.1.24. Trp-Trp-Gly-OBzl (**4b**)*

Using the same procedure as described for Trp-Trp-Ala-OBzl from 500 mg (0.79 mmol) of Boc-Trp-Trp-Gly-OBzl 446 mg (99%) of the title compound was obtained as colorless powder. Mp 201–203 °C; ESI/MS (*m*/*e*) 538 $[M + H]^+$; $[\alpha]_D^{20} = 8.23$ (*c* 1.2, CH_3OH); ^1H NMR (500 MHz, DMSO-d_6) δ/ppm = 10.96 (s, 1H), 10.90 (s, 1H), 8.80 (d, $J = 7.3$ Hz, 1H), 8.67 (d, $J = 8.3$ Hz, 1H), 7.60 (d, $J = 7.9$ Hz, 1H), 7.52 (d, $J = 7.9$ Hz, 1H), 7.17 (m, 13H), 5.05 (m, 2H), 4.70 (m, 2H), 3.16 (m, 6H), 2.02 (s, 2H); ^{13}C NMR (125 MHz, DMSO-d_6) δ/ppm = 172.9, 142.2, 136.7, 130.2, 127.7, 127.5, 127.2, 122.9, 122.2, 120.1, 119.2, 119.0, 111.3, 111.1, 110.9, 68.5, 54.6, 48.8, 43.1, 31.4, 30.6. Anal. Calcd for $C_{31}H_{31}N_5O_4$: C, 69.26; H, 5.81; N, 13.30. Found: C, 69.27; H, 5.95; N, 13.52.

*4.1.25. Trp-Trp-Phe-OBzl (**4c**)*

Using the same procedure as described for Trp-Trp-Ala-OBzl from 500 mg (0.69 mmol) of Boc-Trp-Trp-Phe-OBzl 432 mg (97%)

of the title compound was obtained as colorless powder. Mp 199–201 °C; ESI/MS (*m*/*e*) 628 $[M + H]^+$; $[\alpha]_D^{20}$ = 11.23 (*c* 1.1, CH_3OH); ^1H NMR (500 MHz, DMSO-d_6) δ/ppm = 10.98 (m, 2H), 8.98 (d, *J* = 8.0 Hz, 1H), 8.82 (d, *J* = 7.2 Hz, 1H), 7.64 (d, *J* = 7.9 Hz, 1H), 7.53 (d, *J* = 11.4 Hz, 1H), 7.19 (m, 18H), 5.03 (m, 2H), 4.68 (m, 2H), 4.41 (m, 1H), 3.10 (m, 6H), 1.98 (s, 2H); ^{13}C NMR (125 MHz, DMSO-d_6) δ/ppm = 172.9, 142.2, 139.6, 136.7, 130.0, 128.6, 127.8, 127.5, 127.2, 126.1, 122.9, 122.2, 120.1, 119.2, 119.0, 111.3, 111.1, 110.9, 68.6, 54.6, 53.7, 40.6, 31.2, 30.6. Anal. Calcd for $C_{38}H_{37}N_5O_4$: C, 72.71; H, 5.94; N, 11.16. Found: C, 72.50; H, 5.80; N, 11.39.

4.1.26. Trp-Trp-Leu-OBzl (**4d**)

Using the same procedure as described for Trp-Trp-Ala-OBzl from 500 mg (0.72 mmol) of Boc-Trp-Trp-Leu-OBzl 450 mg (99%) of the title compound was obtained as colorless powder. Mp 222–224 °C; ESI/MS (*m*/*e*) 594 $[M + H]^+$; $[\alpha]_D^{20}$ = 15.76 (*c* 1.3, CH_3OH); ^1H NMR (500 MHz, DMSO-d_6) δ/ppm = 10.92 (m, 2H), 8.76 (d, *J* = 8.1 Hz, 1H), 8.71 (d, *J* = 7.2 Hz, 1H), 7.64 (d, *J* = 7.9 Hz, 1H), 7.50 (d, *J* = 7.9 Hz, 1H), 7.16 (m, 13H), 6.85 (s, 2H), 5.02 (m, 2H), 4.63 (m, 2H), 3.75 (m, 1H), 3.15 (m, 4H), 2.01 (s, 2H), 1.59 (m, 1H), 0.89 (m, 6H); ^{13}C NMR (125 MHz, DMSO-d_6) δ/ppm = 172.9, 142.2, 136.8, 130.1, 127.8, 127.5, 127.1, 122.9, 122.2, 120.1, 119.2, 119.0, 111.3, 111.1, 110.9, 68.6, 54.8, 51.3, 43.6, 31.3, 30.6, 22.6, 22.0. Anal. Calcd for $C_{35}H_{39}N_5O_4$: C, 70.80; H, 6.62; N, 11.80. Found: C, 70.98; H, 6.77; N, 12.03.

4.1.27. Trp-Trp-Ile-OBzl (**4e**)

Using the same procedure as described for Trp-Trp-Ala-OBzl from 500 mg (0.72 mmol) of Boc-Trp-Trp-Ile-OBzl 429 mg (99%) of the title compound was obtained as colorless powder. Mp 228–230 °C; ESI/MS (*m*/*e*) 594 $[M + H]^+$; $[\alpha]_D^{20}$ = 17.00 (*c* 1.2, CH_3OH); ^1H NMR (500 MHz, DMSO-d_6) δ/ppm = 10.96 (m, 2 H), 8.70 (d, *J* = 7.2 Hz, 1H), 8.65 (d, *J* = 8.0 Hz, 1H), 7.25 (m, 13H), 6.82 (s, 2H), 5.04 (m, 2H), 4.68 (m, 2H), 3.47 (m, 1H), 3.11 (m, 4H), 1.98 (s, 2H), 1.25 (m, 1H), 1.08 (m, 2H), 0.83 (m, 6H); ^{13}C NMR (125 MHz, DMSO-d_6) δ/ppm = 172.9, 142.1, 136.6, 130.0, 127.8, 127.5, 127.2, 122.8, 122.2, 120.1, 119.2, 119.0, 111.3, 111.1, 110.9, 68.6, 57.1, 54.8, 39.5, 31.2, 30.6, 24.9, 14.6, 10.9. Anal. Calcd for $C_{35}H_{39}N_5O_4$: C, 70.80; H, 6.62; N, 11.80. Found: C, 71.01; H, 6.78; N, 11.58.

4.1.28. Trp-Trp-Val-OBzl (**4f**)

Using the same procedure as described for Trp-Trp-Ala-OBzl from 500 mg (0.74 mmol) of Boc-Trp-Trp-Val-OBzl 440 mg (97%) of the title compound was obtained as colorless powder. Mp 200–202 °C; ESI/MS (*m*/*e*) 580 $[M + H]^+$; $[\alpha]_D^{20}$ = 13.43 (*c* 1.4, CH_3OH); ^1H NMR (500 MHz, DMSO-d_6) δ/ppm = 10.90 (m, 2H), 8.72 (d, *J* = 7.3 Hz, 1H), 8.58 (d, *J* = 7.9 Hz, 1H), 8.63 (d, *J* = 7.9 Hz, 1H), 7.49 (d, *J* = 7.9 Hz, 1H), 7.17 (m, 13H), 5.03 (m, 2H), 4.71 (dd, *J* = 13.5 Hz, *J* = 5.4 Hz, 1H), 4.62 (dd, *J* = 14.3 Hz, *J* = 7.1 Hz, 1H), 3.61 (m, 1H), 3.17 (m, 4H), 2.07 (m, 1H), 1.98 (s, 2H), 0.90 (m, 6H); ^{13}C NMR (125 MHz, DMSO-d_6) δ/ppm = 172.9, 142.1, 136.7, 130.0, 127.7, 127.5, 127.2, 122.9, 122.2, 120.1, 119.2, 119.0, 111.3, 111.1, 110.9, 68.5, 59.7, 54.8, 33.6, 31.2, 30.7, 17.4. Anal. Calcd for $C_{34}H_{37}N_5O_4$: C, 70.45; H, 6.34; N, 12.08. Found: C, 70.26; H, 6.20; N, 11.89.

4.1.29. Trp-Trp-Ser-OBzl (**4g**)

Using the same procedure as described for Trp-Trp-Ala-OBzl from 500 mg (0.75 mmol) of Boc-Trp-Trp-Ser-OBzl 440 mg (97%) of the title compound was obtained as colorless powder. Mp 218–220 °C; ESI/MS (*m*/*e*) 568 $[M + H]^+$; $[\alpha]_D^{20}$ = 25.37 (*c* 1.3, CH_3OH); ^1H NMR (500 MHz, DMSO-d_6) δ/ppm = 10.93 (m, 2H), 8.72 (m, 2H), 7.28 (m, 15H), 5.09 (m, 2H), 4.61 (m, 2H), 4.08 (m, 2H), 3.46 (m, 1H), 3.13 (m, 4H), 2.06 (s, 2H), 1.98 (s, 1H); ^{13}C NMR (125 MHz, DMSO-d_6) δ/ppm = 172.7, 142.1, 136.8, 130.1, 127.6, 127.5, 127.1, 122.9, 122.2, 120.1, 119.2, 119.0, 111.4, 111.1, 110.9, 68.6, 64.1, 56.8, 54.7, 31.4, 30.6. Anal. Calcd for $C_{32}H_{33}N_5O_5$: C, 67.71; H, 5.86; N, 12.34. Found: C, 67.50; H, 5.71; N, 12.11.

4.1.30. Trp-Trp-Thr-OBzl (**4h**)

Using the same procedure as described for Trp-Trp-Ala-OBzl from 500 mg (0.73 mmol) of Boc-Trp-Trp-Thr-OBzl 429 mg (95%) of the title compound was obtained as colorless powder. Mp 195–197 °C; ESI/MS (*m*/*e*) 582 $[M + H]^+$; $[\alpha]_D^{20}$ = 6.10 (*c* 1.2, CH_3OH); ^1H NMR (500 MHz, DMSO-d_6) δ/ppm = 10.97 (m, 2H), 7.32 (m, 15H), 6.76 (s, 2H), 5.07 (m, 2H), 4.66 (m, 2H), 3.62 (m, 1H), 3.40 (m, 2H), 3.13 (m, 4H), 1.98 (s, 2H), 1.15 (m, 3H); ^{13}C NMR (125 MHz, DMSO-d_6) δ/ppm = 172.9, 142.3, 136.8, 130.1, 127.7, 127.5, 127.2, 122.9, 122.2, 120.1, 119.2, 119.0, 111.4, 111.1, 110.9, 71.0, 68.6, 65.8, 54.6, 31.3, 30.8, 19.2. Anal. Calcd for $C_{33}H_{35}N_5O_5$: C, 68.14; H, 6.07; N, 12.04. Found: C, 68.35; H, 6.22; N, 12.25.

4.1.31. Trp-Trp-Tyr-OBzl (**4i**)

Using the same procedure as described for Trp-Trp-Ala-OBzl from 500 mg (0.67 mmol) of Boc-Trp-Trp-Tyr-OBzl 449 mg (98%) of the title compound was obtained as colorless powder. Mp 207–209 °C; ESI/MS (*m*/*e*) 644 $[M + H]^+$; $[\alpha]_D^{20}$ = 9.77 (*c* 1.1, CH_3OH); ^1H NMR (500 MHz, DMSO-d_6) δ/ppm = 10.89 (m, 2H), 8.78 (d, *J* = 7.3 Hz, 1H), 8.74 (d, *J* = 8.2 Hz, 1H), 7.66 (d, *J* = 8.0 Hz, 1H), 7.51 (d, *J* = 7.9 Hz, 1H), 7.07 (m, 17H), 5.90 (s, 1H), 5.02 (m, 2 H), 4.70 (m, 2H), 3.90 (m, 1H), 3.04 (m, 6H), 1.98 (s, 2H); ^{13}C NMR (125 MHz, DMSO-d_6) δ/ppm = 172.6, 155.9, 142.2, 136.7, 132.2, 130.1, 129.0, 127.7, 127.5, 127.2, 122.9, 122.2, 120.1, 119.2, 119.0, 115.2, 111.3, 111.1, 110.9, 68.6, 54.8, 53.1, 40.6, 31.3, 30.8. Anal. Calcd for $C_{38}H_{37}N_5O_5$: C, 70.90; H, 5.79; N, 10.88. Found: C, 70.69; H, 5.63; N, 11.12.

4.1.32. Trp-Trp-Pro-OBzl (**4j**)

Using the same procedure as described for Trp-Trp-Ala-OBzl from 500 mg (0.74 mmol) of Boc-Trp-Trp-Pro-OBzl 451 mg (99%) of the title compound was obtained as colorless powder. Mp 182–184 °C; ESI/MS (*m*/*e*) 578 $[M + H]^+$; $[\alpha]_D^{20}$ = 16.73 (*c* 1.3, CH_3OH); ^1H NMR (500 MHz, DMSO-d_6) δ/ppm = 10.92 (s, 1H), 10.87 (s, 1H), 8.73 (m, 2H), 7.64 (d, *J* = 7.9 Hz, 1H), 7.50 (d, *J* = 7.9 Hz, 1H), 7.18 (m, 13H), 5.06 (m, 2H), 4.66 (m, 2H), 4.08 (m, 1H), 3.16 (m, 6H), 2.02 (m, 1H), 1.79 (m, 4H); ^{13}C NMR (125 MHz, DMSO-d_6) δ/ppm = 172.7, 142.2, 136.6, 130.1, 127.8, 127.5, 127.2, 122.9, 122.2, 120.1, 119.2, 119.0, 111.3, 111.1, 110.9, 68.7, 60.5, 54.8, 45.7, 32.3, 31.2, 30.6, 24.9. Anal. Calcd for $C_{34}H_{35}N_5O_4$: C, 70.69; H, 6.11; N, 12.12. Found: C, 70.90; H, 6.27; N, 12.34.

4.1.33. Trp-Trp-Met-OBzl (**4k**)

Using the same procedure as described for Trp-Trp-Ala-OBzl from 500 mg (0.70 mmol) of Boc-Trp-Trp-Met-OBzl 448 mg (98%) of the title compound was obtained as colorless powder. Mp 215–217 °C; ESI/MS (*m*/*e*) 612 $[M + H]^+$; $[\alpha]_D^{20}$ = 7.77 (*c* 1.4, CH_3OH); ^1H NMR (500 MHz, DMSO-d_6) δ/ppm = 10.96 (m, 2H), 8.79 (d, *J* = 7.3 Hz, 1H), 8.71 (d, *J* = 7.9 Hz, 1H), 7.72 (d, *J* = 7.8 Hz, 1H), 7.67 (d, *J* = 7.8 Hz, 1H), 7.19 (m, 13H), 5.03 (m, 2H), 4.71 (dd, *J* = 14.2 Hz, *J* = 7.3 Hz, 1H), 4.63 (dd, *J* = 14.2 Hz, *J* = 7.3 Hz, 1H), 3.19 (m, 5H), 2.03 (m, 3 H), 1.98 (s, 2 H), 1.62 (m, 4 H); ^{13}C NMR (125 MHz, DMSO-d_6) δ/ppm = 172.9, 142.0, 136.9, 130.2, 127.7, 127.5, 127.2, 122.9, 122.2, 120.1, 119.2, 119.0, 111.3, 111.1, 110.8, 68.6, 54.9, 53.2, 34.5, 31.4, 30.6, 29.5, 17.8. Anal. Calcd for $C_{34}H_{37}N_5O_4S$: C, 66.75; H, 6.10; N, 11.45. Found: C, 66.94; H, 6.25; N, 11.23.

4.1.34. Trp-Trp-Glu(OBzl)-OBzl (**4l**)

Using the same procedure as described for Trp-Trp-Ala-OBzl from 500 mg (0.63 mmol) of Boc-Trp-Trp-Glu(OBzl)-OBzl 455 mg (99%) of the title compound was obtained as colorless powder. Mp 214–216 °C; ESI/MS (*m*/*e*) 700 $[M + H]^+$; $[\alpha]_D^{20}$ = 20.17 (*c* 1.1, CH_3OH); ^1H NMR (500 MHz, DMSO-d_6) δ/ppm = 10.93 (m, 2H), 8.77

(d, J = 7.2 Hz, 1H), 8.73 (d, J = 7.7 Hz, 1H), 7.64 (d, J = 7.8 Hz, 1H), 7.50 (d, J = 7.8 Hz, 1H), 7.16 (m, 18H), 5.03 (m, 4H), 4.68 (m, 2 H), 3.82 (m, 1H), 3.07 (m, 4H), 2.56 (m, 2H), 2.06 (m, 2H), 1.98 (s, 2H); ^{13}C NMR (125 MHz, DMSO-d_6) δ/ppm = 173.3, 172.7, 142.5, 136.8, 130.1, 129.0, 127.7, 127.5, 127.2, 122.9, 122.2, 120.1, 119.2, 119.0, 111.3, 111.1, 110.9, 68.6, 54.8, 53.6, 31.3, 30.6, 29.2, 27.8. Anal. Calcd for $C_{41}H_{41}N_5O_6$: C, 70.37; H, 5.91; N, 10.01. Found: C, 70.16; H, 5.75; N, 10.24.

4.1.35. Trp-Trp-Asp(OBzl)-OBzl (**4m**)

Using the same procedure as described for Trp-Trp-Ala-OBzl from 500 mg (0.64 mmol) of Boc-Trp-Trp-Asp(OBzl)-OBzl 450 mg (98%) of the title compound was obtained as colorless powder. Mp 210–212 °C; ESI/MS (m/e) 686 $[M + H]^+$; $[\alpha]_D^{20}$ = 10.03 (c 1.2, CH_3OH); ^{1}H NMR (500 MHz, DMSO-d_6) δ/ppm = 10.98 (m, 2H), 8.77 (d, J = 7.9 Hz, 1H), 7.72 (d, J = 7.3 Hz, 1H), 7.30 (m, 20H), 5.08 (m, 4H), 4.65 (m, 2H), 3.36 (m, 1H), 3.17 (m, 4H), 2.92 (m, 2H), 1.99 (s, 2H); ^{13}C NMR (125 MHz, DMSO-d_6) δ/ppm = 173.4, 172.9, 142.3, 141.1, 136.8, 130.2, 129.1, 127.8, 127.6, 127.3, 122.9, 122.2, 120.1, 119.2, 119.0, 111.3, 111.1, 110.9, 68.7, 54.5, 49.3, 41.0, 31.3, 30.2. Anal. Calcd for $C_{40}H_{39}N_5O_6$: C, 70.06; H, 5.73; N, 10.21. Found: C, 70.25; H, 5.90; N, 10.43.

4.1.36. Trp-Trp-Cys(4-MeOBzl)-OBzl (**4n**)

Using the same procedure as described for Trp-Trp-Ala-OBzl from 500 mg (0.62 mmol) of Boc-Trp-Trp-Cys(4-OMeBzl)-OBzl 441 mg (96%) of the title compound was obtained as colorless powder. Mp 219–221 °C; ESI/MS (m/e) 704 $[M + H]^+$; $[\alpha]_D^{20}$ = 14.43 (c 1.5, CH_3OH); ^{1}H NMR (500 MHz, DMSO-d_6) δ/ppm = 10.99 (m, 2H), 8.93 (d, J = 7.9 Hz, 1H), 8.75 (d, J = 7.9 Hz, 1H), 7.63 (d, J = 7.9 Hz, 1 H), 7.44 (d, J = 7.9 Hz, 1H), 7.10 (m, 17H), 4.98 (m, 2H), 4.72 (dd, J = 10.5 Hz, J = 7.5 Hz, 1H), 4.60 (dd, J = 10.5 Hz, J = 7.5 Hz, 1H), 3.71 (m, 5H), 3.43 (dd, J = 10.5 Hz, J = 7.5 Hz, 1 H), 3.00 (m, 6 H), 1.98 (s, 2H); ^{13}C NMR (125 MHz, DMSO-d_6) δ/ppm = 172.7, 159.2, 142.2, 136.7, 130.1, 129.9, 129.3, 127.7, 127.5, 127.2, 122.9, 122.2, 120.1, 119.2, 119.0, 114.0, 111.3, 111.1, 110.9, 68.6, 56.2, 54.7, 54.4, 38.4, 36.7, 31.3, 30.7. Anal. Calcd for $C_{40}H_{41}N_5O_5S$: C, 68.26; H, 5.87; N, 9.95. Found: C, 68.04; H, 5.71; N, 10.17.

4.1.37. Trp-Trp-Arg(N^GNO_2)-OBzl (**4o**)

Using the same procedure as described for Trp-Trp-Ala-OBzl from 500 mg (0.64 mmol) of Boc-Trp-Trp-Arg(N^GNO_2)-OBzl 445 mg (97%) of the title compound was obtained as colorless powder. Mp 188–190 °C; ESI/MS (m/e) 682 $[M + H]^+$; $[\alpha]_D^{20}$ = 18.00 (c 1.5, CH_3OH); ^{1}H NMR (500 MHz, DMSO-d_6) δ/ppm = 11.00 (m, 2H), 8.53 (d, J = 7.5 Hz, 1H), 8.39 (d, J = 7.4 Hz, 1H), 7.34 (m, 15H), 5.10 (m, 2H), 4.19 (m, 1H), 4.04 (m, 2H), 3.14 (m, 4H), 1.73 (m, 2H), 2.02 (s, 2H), 1.95 (m, 3H), 1.58 (m, 4H); ^{13}C NMR (125 MHz, DMSO-d_6) δ/ppm = 172.6, 163.1, 142.2, 136.7, 130.1, 127.7, 127.5, 127.2, 122.9, 122.2, 120.1, 119.2, 119.0, 111.3, 111.1, 110.9, 68.5, 54.7, 53.7, 37.5, 31.8, 31.3, 30.5, 24.7.Anal. Calcd for $C_{35}H_{39}N_9O_6$: C, 61.66; H, 5.77; N, 18.49. Found: C, 61.84; H, 5.93; N, 18.26.

4.1.38. Trp-Trp-Lys(N^{ω}-Z)-OBzl (**4p**)

Using the same procedure as described for Trp-Trp-Ala-OBzl from 500 mg (0.59 mmol) of Boc-Trp-Trp-Lys(N^{ω}-Z)-OBzl 459 mg (99%) of the title compound was obtained as colorless powder. Mp 193–195 °C; ESI/MS (m/e) 743 $[M + H]^+$; $[\alpha]_D^{20}$ = 14.77 (c 1.2, CH_3OH); ^{1}H NMR (500 MHz, DMSO-d_6) δ/ppm = 10.99 (m, 2H), 8.97 (d, J = 7.9 Hz, 1H), 8.66 (d, J = 7.3 Hz, 1H), 8.26 (d, J = 7.1 Hz, 1H), 7.78 (d, J = 7.9 Hz, 1H), 7.64 (d, J = 7.9 Hz, 1H), 7.17 (m, 18 H), 5.01 (m, 4 H), 4.72 (m, 1 H), 4.33 (m, 1 H), 3.36 (m, 1H), 3.04 (m, 6H), 1.99 (s, 2H), 1.50 (m, 6H); ^{13}C NMR (125 MHz, DMSO-d_6) δ/ppm = 172.9, 156.1, 142.2, 141.1, 136.7, 130.1, 129.3, 127.7, 127.5, 127.2, 122.9, 122.2, 120.1, 119.2, 119.0, 111.3, 111.1, 110.9, 68.6, 65.5, 54.8, 54.1, 42.2, 34.6, 31.3, 30.5, 29.6. Anal. Calcd for $C_{43}H_{46}N_6O_6$: C, 69.52; H, 6.24; N, 11.31. Found: C, 69.30; H, 6.10; N, 11.54.

4.1.39. Trp-Trp-Gln-OBzl (**4q**)

Using the same procedure as described for Trp-Trp-Ala-OBzl from 500 mg (0.71 mmol) of Boc-Trp-Trp-Gln-OBzl 424 mg (93%) of the title compound was obtained as colorless powder. Mp 188–190 °C; ESI/MS (m/e) 609 $[M + H]^+$; $[\alpha]_D^{20}$ = 13.33 (c 1.4, CH_3OH); ^{1}H NMR (500 MHz, DMSO-d_6) δ/ppm = 10.88 (m, 2H), 8.75 (d, J = 7.2 Hz, 1H), 8.70 (d, J = 7.8 Hz, 1H), 7.56 (m, 2H), 7.16 (m, 13H), 6.17 (s, 2H), 5.03 (m, 2H), 4.68 (m, 2H), 3.89 (m, 1H), 3.16 (m, 4H), 2.26 (m, 2H), 2.05 (s, 2H), 1.98 (m, 2H); ^{13}C NMR (125 MHz, DMSO-d_6) δ/ppm = 174.2, 172.9, 142.4, 136.8, 130.1, 127.7, 127.5, 127.2, 122.9, 122.2, 120.1, 119.2, 119.0, 111.3, 111.1, 110.9, 68.7, 54.6, 53.7, 32.4, 31.3, 30.5, 30.2. Anal. Calcd for $C_{34}H_{36}N_6O_5$: C, 67.09; H, 5.96; N, 13.81. Found: C, 66.88; H, 5.81; N, 13.60.

4.1.40. Trp-Trp-Asn-OBzl (**4r**)

Using the same procedure as described for Trp-Trp-Ala-OBzl from 500 mg (0.72 mmol) of Boc-Trp-Trp-Asn-OBzl 431 mg (95%) of the title compound was obtained as colorless powder. Mp 199–201 °C; ESI/MS (m/e) 595 $[M + H]^+$; $[\alpha]_D^{20}$ = 8.13 (c 1.1, CH_3OH); ^{1}H NMR (500 MHz, DMSO-d_6) δ/ppm = 10.96 (m, 2H), 8.74 (m, 2H), 7.59 (m, 2H), 7.21 (m, 13H), 6.18 (s, 2H), 5.05 (m, 2H), 4.62 (m, 2H), 2.98 (m, 7H), 1.96 (s, 2H); ^{13}C NMR (125 MHz, DMSO-d_6) δ/ppm = 174.7, 172.6, 142.3, 136.7, 130.1, 127.7, 127.5, 127.2, 122.9, 122.2, 120.1, 119.2, 119.0, 111.3, 111.1, 110.9, 68.9, 54.5, 49.3, 40.3, 31.0, 30.5. Anal. Calcd for $C_{33}H_{34}N_6O_5$: C, 66.65; H, 5.76; N, 14.13. Found: C, 66.44; H, 5.61; N, 14.35.

4.1.41. Trp-Trp-His-OBzl (**4s**)

Using the same procedure as described for Trp-Trp-Ala-OBzl from 500 mg (0.70 mmol) of Boc-Trp-Trp-His-OBzl 320 mg (70%) of the title compound was obtained as colorless powder. Mp 211–213 °C; ESI/MS (m/e) 618 $[M + H]^+$; $[\alpha]_D^{20}$ = 16.43 (c 1.5, CH_3OH); ^{1}H NMR (500 MHz, DMSO-d_6) δ/ppm = 11.03 (s, 1H), 10.98 (s, 1H), 9.02 (s, 1H), 8.90 (m, 2H), 8.43 (s, 3H), 7.66 (d, J = 7.9 Hz, 1H), 7.52 (d, J = 7.9 Hz, 1H), 7.29 (m, 13H), 5.05 (m, 2H), 4.66 (m, 2H), 3.20 (m, 6H), 2.98 (m, 1H), 2.02 (s, 2 H); ^{13}C NMR (125 MHz, DMSO-d_6) δ/ppm = 172.6, 142.0, 136.5, 135.4, 133.6, 130.1, 127.7, 127.5, 127.2, 122.9, 122.2, 120.1, 119.8, 119.2, 119.0, 111.3, 111.1, 110.8, 68.6, 54.5, 53.3, 33.0, 31.2, 30.9. Anal. Calcd for $C_{35}H_{35}N_7O_4$: C, 68.06; H, 5.71; N, 15.87. Found: C, 67.85; H, 5.55; N, 15.63.

4.1.42. Trp-Trp-Trp-OBzl (**4t**)

Using the same procedure as described for Trp-Trp-Ala-OBzl from 500 mg (0.65 mmol) of Boc-Trp-Trp-Trp-OBzl 416 mg (91%) of the title compound was obtained as colorless powder. Mp 212–214 °C; ESI/MS (m/e) 667 $[M + H]^+$; $[\alpha]_D^{20}$ = −6.73 (c 1.2, CH_3OH); ^{1}H NMR (500 MHz, DMSO-d_6) δ/ppm = 11.10 (m, 3H), 8.03 (m, 2H), 7.39 (m, 20H), 4.57 (m, 4H), 3.59 (s, 1H), 3.43 (m, 6H), 2.05 (s, 2H); ^{13}C NMR (125 MHz, DMSO-d_6) δ/ppm = 172.8, 142.2, 136.7, 136.3, 130.1, 127.7, 127.5, 127.2, 122.9, 122.2, 120.1, 119.2, 119.0, 111.3, 111.1, 110.9, 68.5, 55.0, 54.7, 34.1, 31.3, 30.7. Anal. Calcd for $C_{40}H_{38}N_6O_4$: C, 72.05; H, 5.74; N, 12.60. Found: C, 71.86; H, 5.60; N, 12.82.

4.2. Bioassay

4.2.1. In vitro anti-proliferation assay of **4a**–**t**

Following a slightly modified procedure [13] the *in vitro* anti-proliferation assays were carried out by use of 96 microtiter plate cultures and MTT staining. The $HepG_2$, S180, H22, K562 and B16 cells (final concentration in the growth medium was 1×10^4/ml) were grown in RPMI-1640 medium or DMEM medium (containing 10%, v/v FCS), penicillin (100 μg/ml) and streptomycin (100 μg/ml) without (for control) or with **4a**–**t** (final concentrations ranging from 1 μM). The cultures were propagated at 37 °C in a humidified atmosphere containing 5% CO_2 for 24 h, after the first renew of the

growth medium without (for control) or with **4a**–**t** (for test sample) were propagated for another 48 h, after the second renew of the growth medium with 25 μl of MTT solution (5 mg/ml) were propagated for another 4 h. The growth medium was removed and the residue was dried in the air. The dried residues were dissolved in 100 μl of DMSO and the absorption values of light of the formed purple solutions were recorded on Bio-rad 570 nm microplate (Bio-rad, USA). The inhibited rates were calculated according to I% = % (C − T/C).

*4.2.2. In vivo anti-tumor assay of **4a**–**t***

The assessments described here were performed based on a protocol reviewed and approved by the ethics committee of Capital Medical University. The committee assures the welfare of the male ICR mice was maintained in accordance to the requirements of the animal welfare act and according to the guide for care and use of laboratory animals. The mice, purchased from Peking University Health Science Center, were 10–12 weeks old at the beginning of the experiments. S180 cells for the initiation of subcutaneous tumors were obtained from the ascitic form of the tumors in mice and serially transplanted once per week. Subcutaneous tumors were implanted by injecting 0.2 ml of NS containing 1×10^7 viable tumor cells under the skin on the right oxter of the mice. Twenty-four hours after the implantation the tumor-bearing mice were randomized into 22 experimental groups (12 per group). All the mice were given a daily i.p. injection of cytarabine and doxorubicin (positive control, 2.0 μmol/kg/day in 0.2 ml of NS), or NS (negative control, 0.2 ml), or **4a**–**t** (8.9 μmol/kg/day in 0.2 ml of NS) for seven consecutive days. Twenty-four hours after the last i.p. injection, all mice were sacrificed by diethyl ether anesthesia, the tumors of the treated (T_w) and control (C_w) groups were separated and weighed to calculate the percentage of the tumor growth inhibition by using the following equation:

$$\text{Inhibition}\ (\%) = [1 - (T_w/C_w)] \times 100$$

*4.2.3. In vivo dose-dependent assay of **4f***

Male ICR mice, purchased from Peking University Health Science Center, were 10–12 week old at the beginning of the experiments. The tumor used was S180 that forms solid tumors, when injected subcutaneously. S180 cells for initiation of the subcutaneous tumors were obtained from the ascitic form of the tumors in the mice, which were serially transplanted once per week. Subcutaneous tumors were implanted by injecting 1×10^7 viable tumor cells in 0.2 ml of NS under the skin of the right oxter of the mice. Twenty-four hours after the implantation, the mice were randomized into 6 experimental groups (10 per group), and were given a daily i.p. injection of cytarabine (positive control, 8.9, 0.89 or 0.089 μmol/kg/day in 0.2 ml of NS), or NS (negative control, 0.2 ml), or **4f** (8.9, 0.89 or 0.089 μmol/kg/day in 0.2 ml of NS) for seven consecutive days. Twenty-four hours after the last i.p. injection, all mice were sacrificed by diethyl ether anesthesia, the tumors of the treated (T_w) and control (C_w) groups were separated and weighed to calculate the percentage of the tumor growth inhibition accordingly.

4.2.4. In vivo acute toxicity assay

Health male ICR mice of 24-week old were given a single i.p injection of 500 mg/kg of the anti-tumoral active **4a**–**c**,**e**–**l**,**n**–**s** in 0.2 ml of NS. The mice were monitored for 7 days to observe the neurotoxic behavior, such as tremor, twitch, jumping, tetanus, and supination, as well as the death. On the 7th day the survival mice were sacrificed by diethyl ether anesthesia and dissected to immediately obtain the organs for examination.

Acknowledgments

This work was completed in the Beijing area major laboratory of peptide and small molecular drugs, supported by PHR (IHLB, KM 200910025009, KM200910025010), the National Natural Scientific Foundation of China (81072522), and Special Project (2011ZX09302-007-01) of China.

References

[1] G. Momekov, A. Bakalova, M. Karavanova, Curr. Med. Chem. 12 (2005) 2177–2191.
[2] A. Bolognese, G. Correale, M. Manfra, A. Lavecchia, O. Mazzoni, E. Novellino, P. La Colla, G. Sanna, R. Loddo, J. Med. Chem. 47 (2004) 849–858.
[3] M.A. Lynch, O. Duval, A. Sukhanova, J. Devy, S.P. Mackay, R.D. Waigh, I. Nabiev, Bioorg. Med. Chem. Lett. 11 (2001) 2643–2646.
[4] R. Cao, W. Peng, H. Chen, Y. Ma, X. Liu, X. Hou, H. Guan, A. Xu, Biochem. Biophys. Res. Commun. 338 (2005) 1557–1563.
[5] M. Laronze, M. Boisbrun, S. Leonce, B. Pfeiffer, P. Renard, O. Lozach, L. Meijer, A. Lansiaux, C. Bailly, J. Sapi, J.Y. Laronze, Bioorg. Med. Chem. 13 (2005) 2263–2283.
[6] A.M. Sobhani, S.A. Ebrahimi, M.J. Mahmoudian, J. Pharm. Pharm. Sci. 5 (2002) 19–23.
[7] M. Zhao, L. Bi, W. Wang, C. Wang, M. Baudy-Floc, J. Ju, S.Q. Peng, Bioorg. Med. Chem. 14 (2006) 6998–7010.
[8] J.H. Wu, M. Zhao, K.D. Qian, K.H. Lee, S.M. Natschke, S.Q. Peng, Eur. J. Med. Chem. 44 (2009) 4153–4161.
[9] Z. Cruz-Monserra, H.C. Vervoot, R. Bai, D.J. Newman, S.B. Howell, G. Los, J.T. Mullaney, M.D. Williams, G.R. Pettit, W. Fenical, E. Hamel, Mol. Pharmacol. 63 (2003) 1273–1280.
[10] J.H. Wu, C.Y. Li, M. Zhao, W.J. Wang, Y.J. Wang, S.Q. Peng, Bioorg. Med. Chem. 18 (2010) 6220–6229.
[11] A.M. Sobhani, S.R. Amini, J.D.A. Tyndall, E. Azizi, M. Daneshtalab, A. Khalaj, J. Mol. Graph. Model. 25 (2006) 459–469.
[12] A. Marco, R.C. Loza-Mejía, L.R. Alfonso, J. Mol. Graph. Model. 27 (2009) 900–907.
[13] C.M.A. Alves, S. Naik, J.P.G. Coutinho, Tetrahedron 65 (2009) 10441–10452.
[14] C.M. Venkatachalam, X. Jiang, T. Oldfield, M. Waldman, J. Mol. Graph. Model. 21 (2003) 289–307.
[15] R.P. Queiroz, M.S.E. Castanheir, C.T.T. Lopes, K.Y. Cruz, G. Kirsch, J. Photochem. Photobiol. A 190 (2007) 45–52.
[16] U. Varadarajan, C. Alfonso, U.N. Balachandran, Polyhedron 26 (2007) 3008–3016.
[17] N. Li, Y. Ma, C. Yang, L.P. Guo, X.R. Yang, Biophys. Chem. 116 (2005) 199–205.
[18] P.U. Maheswari, M. Palaniandavar, J. Inorg. Biochem. 98 (2004) 219–230.
[19] T.S. Pitchumony, H.S. Evans, M. Palaniandavar, J. Inorg. Biochem. 99 (2005) 2110–2118.
[20] F. Arjmand, M. Aziz, Eur. J. Med. Chem. 44 (2009) 834–844.
[21] S. Shi, T. Xie, T.M. Yao, C.R. Wang, X.T. Geng, D.J. Yang, L.J. Han, L.N. Ji, Polyhedron 28 (2009) 1355–1372.
[22] L.W. Hsin, H.P. Wang, P.H. Kao, O. Lee, W.R. Chen, H.W. Chen, J.H. Guh, Y.L. Chan, C.P. His, M.S. Yang, T.K. Li, C.H. Lee, Bioorg. Med. Chem. 16 (2008) 1006–1014.
[23] A.R. Shaikh, M. Ismael, C.A.D. Carpio, H. Tsuboi, M. Koyama, A. Endou, M. Kubo, E. Broclawikc, A. Miyamoto, Bioorg. Med. Chem. Lett. 16 (2006) 5917–5925.
[24] M.R. Doddareddy, Y.S. Cho, H.Y. Koh, A.N. Pae, Bioorg. Med. Chem. 12 (2004) 3977–3985.